

Benchmark Calculation of KRITZ-2 by DRAGON/PARCS

M. Choi, H. Choi, R. Hon

General Atomics: 3550 General Atomics Court, San Diego, CA 92121, USA, Hangbok.Choi@ga.com

Abstract - Benchmark calculations have been conducted for KRITZ-2 Nuclear Energy Agency (NEA) benchmark problems using a reactor simulation code PARCS with lattice parameters generated by DRAGON code and a Monte Carlo code MCNP6. The KRITZ-2 is a small light water reactor with UO₂ and Mixed Oxide (MOX) fuels. The benchmark analyses also examined the fuel assembly modeling by the DRAGON. The PARCS core calculations in conjunction with DRAGON lattice models and ENDF/B-VII Release 1 cross section libraries reproduce the criticality well with a root-mean-square (RMS) of ~0.4% δk . DRAGON/PARCS also predicts the fission rates mostly within ~4%. The MCNP6 results are in general consistent with DRAGON/PARCS results, but with less errors. In particular, the benchmark exercises have shown that it is important to carefully treat the fuel rods located on the core boundary, which have a different neutron moderation effect when compared to the rest of fuel rods.

I. INTRODUCTION

Benchmarking reactor physics codes is an ongoing activity that validates the nuclear data of the reactor design and analysis, methods of generating group constants, models of fuel assembly and reactor core, and the solution method of the reactor calculation. As advanced fuel and reactor concepts are being developed, the physics codes need to be validated for a wide range of design features when compared with conventional reactor concept. The new reactor technology can be successfully developed and deployed only through experimental verifications, including benchmarking the computer codes being used to simulate the reactor operation.

However, building a critical assembly or a demonstration-scale reactor system for the purpose of validating reactor code system is a time-consuming and expensive process. An alternative will be to use an existing data base, which is similar to the system being developed, along with numerical benchmarks based on the most robust computing tools. It is worth noting that the trend in the advanced reactor design is to reduce the core size and to deploy multiple modules, i.e., a small modular reactor (SMR), when compared with conventional large-size reactors. Therefore, unless the computational model explicitly describes fuel rod level details, the typical reactor calculation scheme using the homogenized lattice parameters needs to be reevaluated for the small core analysis.

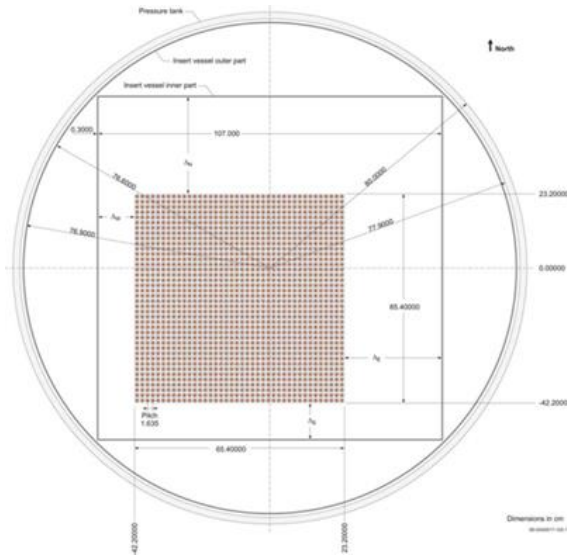
Recently, General Atomics (GA) has installed DRAGON [1] and PARCS [2] codes as main vehicles of the GA Reactor Design System (GARDS) for the advanced reactor design and analysis. Preliminary benchmark calculations have been conducted for KRITZ-2, which is a small, light-water reactor [3]. The Monte Carlo calculations also were conducted in parallel using the model provided by the Nuclear Energy Agency (NEA) benchmark description. It is known that the DRAGON and PARCS have been validated for various thermal reactor problems. Therefore, it may not be necessary to test the physics of those codes. The objective

of this study is to build appropriate fuel assembly model for the group constant generation and to investigate the library group structure that can be used for the UO₂ and Mixed Oxide (MOX) fuel configurations, which is similar to the aim of the NEA KRITZ-2 benchmark. This study is focusing on a small thermal reactor system, which will be expanded to the fast reactor system in the follow-up studies. This paper presents intermediate results of criticality and fission rate calculations produced so far.

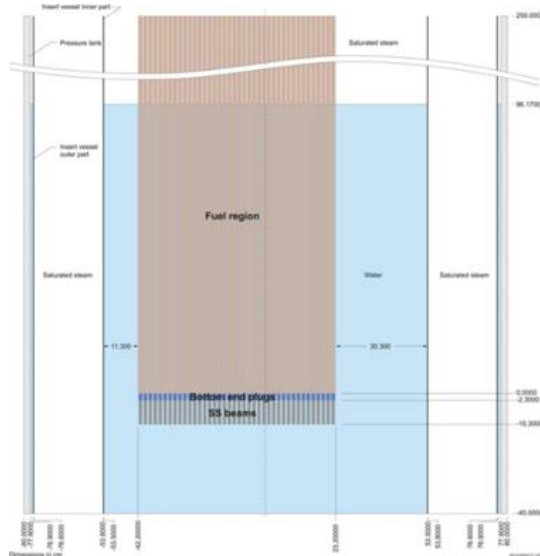
II. BENCHMARK CALCULATION OF KRITZ-2

1. Description of KRITZ-2 Core

The KRITZ reactor consists of light-water-moderated lattices with uranium and/or MOX fuel rods at room temperature and elevated temperatures up to ~245°C. The benchmark problems have been specified for three core configurations: KRITZ-2:1 (KRITZ-LWR-RESR-002), KRITZ-2:13 (KRITZ-LWR-RESR-003), and KRITZ-2:19 (KRITZ-LWR-RESR-001). The reactor consists of a ~5 m high cylindrical pressure tank with a diameter of ~1.5 m, an insert vessel, and a square shape fuel assembly with a side length of ~1 m. Criticality is attained by controlling the boron content in the water and by adjusting the water level. The core configuration is shown in Fig. 1. The key parameters of the critical configurations are summarized in Table I.



(a) KRITZ-2:13 radial layout



(b) KRITZ-2:13 axial layout

Fig. 1. KRITZ-2:13 core configuration [Courtesy of Ref. 3].

2. Computer Codes and Geometry Model

DRAGON (version 4.1.1) is a neutron transport code being developed and maintained by École Polytechnique de Montréal. The code consists of many calculation modules to facilitate implementing new calculation techniques. The current version has the modeling capability of one-dimensional (plane, cylindrical, or spherical), two-dimensional (cartesian or hexagonal), and general three-dimensional geometries so that a single pin, a fuel assembly or bundle, and reactivity devices can be exactly modeled.

PARCS (version 32m17co) is a three-dimensional reactor core simulation code that solves steady-state and time-dependent, multi-group neutron diffusion and transport equations in orthogonal and non-orthogonal geometries.

GenPMAXS (version 6.1.2 dev) [4] is an interface code between a lattice code and PARCS to process burnup-dependent lattice parameters generated by the lattice code into PMAXS format that can be read specifically by the PARCS. At present, several lattice codes, such as HELIOS [5], CASMO [6] and TRITON [7], can be coupled to PARCS through the GenPMAXS. In order to interface lattice parameters generated by the DRAGON to PARCS, new modules have been developed and implemented in the GenPMAXS code so that standard DRAGON output file is converted into a PMAXS format file.

The cross-section libraries are based on ENDF/B-VII Release 1 [8]. Different energy group structures are being tested for the lattice parameter generation by the DRAGON: 69, 172, 361, 586, and 1172 groups. The 69-group is the traditional WIMS library structure. The 172-group is a legacy group structure defined by the UK and France and also adopted by the WIMS library update program of IAEA [9]. The 361-group is an energy mesh defined by Alain Santamarina and Alain Hébert, obtained by refining the group structure of SHEM-281 in the resolved energy domain, above 22.5 eV. The 586 and 1172-group libraries have been developed by GA for application to advanced reactor systems with various neutron spectrum.

Unlike the large commercial reactor, none of the fuel assemblies in the small reactor has the near-reflective boundary condition, and the single-assembly calculation may not be good enough to consider neutron leakage to the assembly boundary which in turn changes the neutron energy distribution. For the fuel assemblies on the core periphery, the color set (CS) model is used to reflect the intra-node neutron transport in the cross-section homogenization. [10, 11]. Figure 2 (b) shows the definition of the supercell model for group constant generation. For the small reactor calculation, the finite difference method (FDM) can be used for the core calculation.

DRAGON models a unit cell or an assembly in both 1-D and 2-D geometry. Figure 2 shows a cartoon of radial configuration of the KRITZ-2 computational model. In order to avoid complex and expensive calculations in CPU times, a few simplifications were made:

- The neutron source, the neutron detectors, and the safety shuttles located in the region between the inner and outer part of the insert vessel shown in Fig. 1 (b) were not modeled.
- The thin annulus between the pressure tank and the insert vessel outer part filled with water up to the same level as the rectangular-shaped inner part was not modeled.

TABLE I. Summary of the critical core specifications

	KRITZ-2:1		KRITZ-2:13		KRITZ-2:19	
	19.7 (°C)	248.5 (°C)	22.1 (°C)	243.0 (°C)	21.1 (°C)	235.9 (°C)
B_z^2 (Buckling)	0.0384	0.025	0.0283	0.0245	0.04	0.028
Fuel rods	UO ₂	UO ₂	UO ₂	UO ₂	PuO ₂ -UO ₂	PuO ₂ -UO ₂
²³⁵ U (wt.%)	1.86	1.86	1.86	1.86	0.16	0.16
PuO ₂ (wt.%)	0.0	0.0	0.0	0.0	1.50	1.50
Number of rods	44 × 44	44 × 44	40 × 40	40 × 40	25 × 24	25 × 24
Lattice pitch (cm)	1.485	1.491	1.635	1.6411	1.8	1.81
Rod Radius (cm)	0.529	0.5302	0.529	0.53015	0.4725	0.4735
Cladding	Zr	Zr	Zr	Zr	Zr	Zr
Inner Radius(cm)	0.5385	0.5392	0.5385	0.5392	0.4725	0.4735
Outer radius(cm)	0.6125	0.6133	0.6125	0.6133	0.5395	0.5402
End-Plugs	Zr	Zr	Zr	Zr	Zr	Zr
Radius (cm)	0.6125	0.6133	0.6125	0.6133	0.4725	0.4731
Height (cm)	2.3	2.303	2.3	2.303	2.3	2.3
Beams	SS-316	SS-316	SS-316	SS-316	SS-316	SS-316
Radius(cm)	0.5	0.502	0.5	0.502	0.5	0.502
Height (cm)	8.0	8.03	8.0	8.03	8.0	8.03
Reflector	water	water	water	water	water	water
Boron (ppm)	217.9	26.2	451.9	280.1	4.8	5.2
Height (cm)	65.28	105.52	96.17	110.96	66.56	100.01
ΔW (cm)	8.1	8.305	11.30	13.14	9.9	10.09
ΔS (cm)	8.1	8.305	11.30	13.14	9.9	10.09
ΔE (cm)	33.56	33.52	30.30	30.26	52.10	52.13
ΔN (cm)	33.56	33.52	30.30	30.26	53.90	54.09

These simplifications were verified to be negligible on k_{eff} in Ref. 3. Therefore, five regions in horizontal direction are modeled for the present DRAGON simulations, as shown in Fig. 2: the fuel region in red, the borated water reflector in light blue, the thin wall of the insert vessel inner region in green, the saturated steam region in grey, and the pressure tank in orange.

3. Lattice Calculation Model

Several DRAGON calculations have been conducted to assess the effect of lattice parameter generation on the criticality calculation. For each lattice model below, cross sections were generated for individual material zone and used for the core criticality calculation. The lattice models are as follows:

Infinite Lattice: One single-fuel assembly and four non-fuel materials (i.e., borated water, thin wall of the inner part of insert vessel, saturated steam, and pressure tank) were all modeled as standalone infinite lattices. The fuel region was modeled with 10×10 pin (unit) cell lattices where one fuel pin was located in each unit cell. Non-fuel regions were modeled as one single-unit lattice with the same height and width as those of a single-fuel assembly.

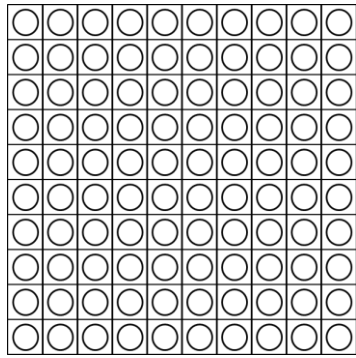
1-D Lattice: The fuel assembly and surrounding non-fuel materials were modeled in 1-D slab model along the mid-line of a core vertical layer. The fuel region was modeled with 20

unit lattices. Non-fuel regions were modeled with one single-unit lattice.

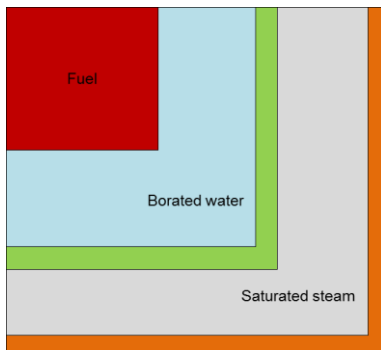
2-D Reduced Lattice: The model consists of one single rectangular fuel assembly surrounded by non-fuel materials. The full core (40×40 fuel rods) was reduced to a 20×20 fuel assembly lattice for KRITZ-2:13. The volume of non-fuel material also was reduced by the fuel assembly volume reduction ratio.

2-D Full Lattice: One quarter of the core was used for the lattice calculation as shown in Figure 2. Fuel assemblies (the red rectangular box in Figure 2) are modeled by 22×22 unit cells for KRITZ-2:1, 20×20 unit cells for KRITZ-2:13, 13×12 unit cells for KRITZ 2:19, respectively.

Both the 2-D reduced and full-lattice models generate material-wise cross sections from the 2-D lattice calculations. For the reduced lattice, all four sides of the fuel assembly have interface with water reflector, while the full lattice has only two interfacing sides, which could result in a slight difference in cross sections of the material around the fuel-reflector interface.



(a) Single-fuel assembly model



(b) Multi-cell model for 2-D full lattice

Fig. 2. DRAGON lattice model.

4. Core Calculation Model

To perform full-core calculations by PARCS, axial geometry of the KRITZ-2 model was divided into five axial levels based on material mixes of the rectangular-shape inner part of the insert vessel. In this axial model, structures above the fuel rods were not explicitly modeled. Vertical fuel lengths are 200 cm for KRITZ-2:1, 250 cm for KRITZ-2:13 and 123.20 cm at 21.1°C, and 123.46 cm at 235.9°C for KRITZ-2:19, respectively.

These five axial regions are marked as Z1, Z2, Z3, Z4, and Z5 in Fig. 3 where Z1 includes only the borated water in the inner part of the insert vessel, Z2 is the beams, Z3 is the end-plug, Z4 is the fuel rods with the borated water between fuel rods (F1), and Z5 is the same fuel rods but with the saturated steam between the fuel rods (F2).

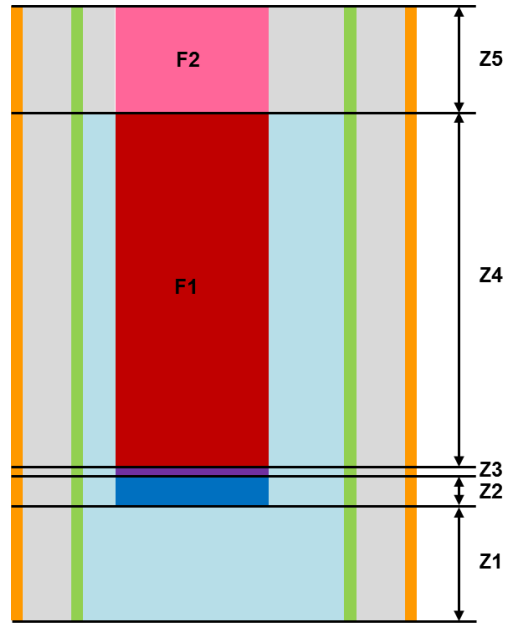
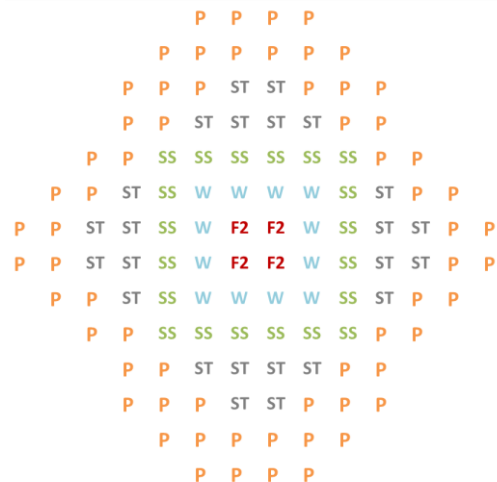
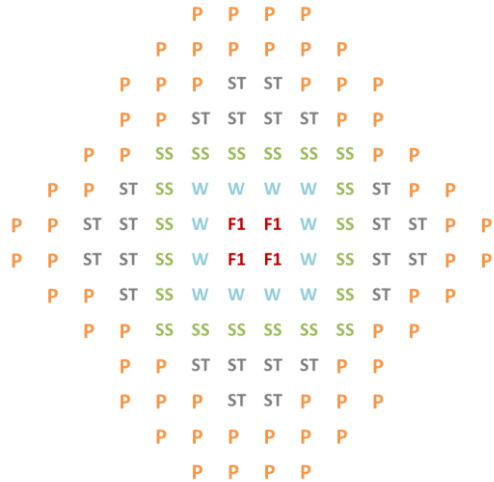


Fig. 3. PARCS axial core model of the KRITZ-2.

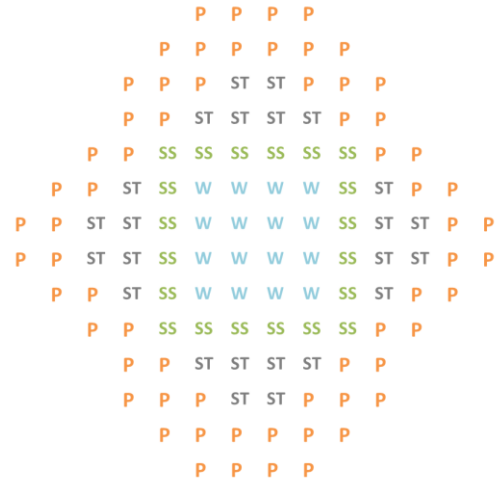
Figure 4 shows radial configuration of PARCS core model at each axial level (Z1, Z2, Z3, Z4 and Z5), where W, SS, ST, P, B, E, F1, and F2 represent the borated water assembly, thin stainless steel wall assembly of the inner part of the insert vessel, saturated steam assembly, pressure tank assembly, beam assembly, end-plug assembly, fuel rod assembly with the borated water between rods, and the fuel assembly with the saturated steam between rods, respectively. As can be seen, four fuel assemblies are combined to build a complete core for each experiment.



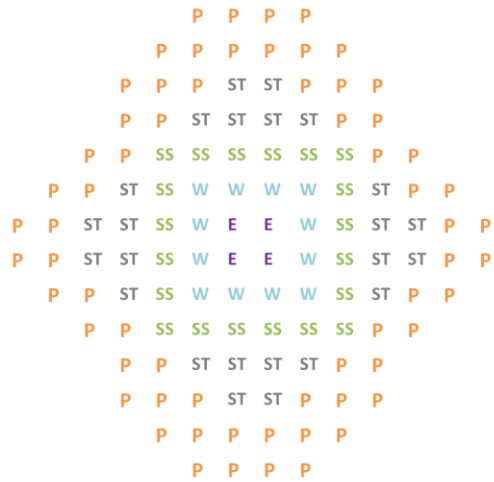
(a) Axial layer Z5



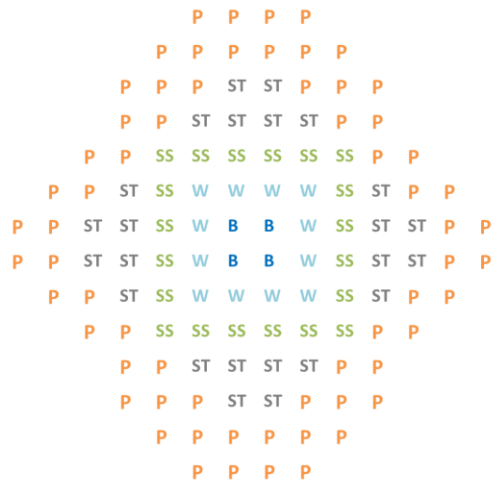
(b) Axial layer Z4



(e) Axial layer Z1



(c) Axial layer Z3



(d) Axial layer Z2

Fig. 4. PARCS radial core model of the KRITZ-2 at each axial layer.

Lattice parameters are computed by DRAGON at each defined axial level (Fig. 3) for each lattice model for the selected KRITZ-2 experiments. Transport calculations were performed by multi-group collision probability method using 361 energy group cross-section SHEM library. For criticality calculations, the fission source eigenvalue problems with B1 method were solved. Since DRAGON does not directly compute transport cross-section data, they were explicitly computed using diffusion cross-section data that was implicitly computed by DRAGON. Computed 361 energy group cross-section data by DRAGON was collapsed into two energy groups (a fast energy and a thermal energy) and also was spatially homogenized over each region, which were converted into the PMAXS format to PARCS via GenPMAXS.

III. SIMULATION RESULTS

1. Core Multiplication Factors

Regarding the lattice model, the test runs have shown that the infinite lattice model is not good for generating the lattice parameters of the systems with high leakage. The 1-D lattice model was constructed from the core center to the physical boundary, and the lattice parameters were generated for individual material zones with critical neutron flux. Though the 1-D lattice model improves the prediction when compared with the infinite lattice model, the average k_{eff} was consistently underestimated. The results of both 2-D reduced and full lattice models, along with the transport cross sections adjusted by the neutron leakage, are close to the measured value. More specifically, the root-mean-square (RMS) error of criticality for the six cases is 0.33% δk and 0.44% δk for the reduced and full-lattice model, respectively. It was also noted that the core calculation based on the reduced-lattice

model slightly over-predicts k_{eff} while that based on the full lattice model slightly under-predicts k_{eff} . In this study, the 2-D full-lattice model is used for the cross-section generation because it is most consistent with actual core configuration.

The criticality calculation results are presented in Table II, where the calculated k_{eff} show good agreements with the experimental values for both the DRAGON/PARCS and MCNP6 calculations. The DRAGON calculation here used SHEM-361 library.

The public cross-section libraries of MCNP6 have limited temperature data. For the principal cross sections, the cross sections of 21°C and 327°C were used for the room and elevated temperatures, respectively. For the $S(\alpha, \beta)$, the elevated temperature of ^{56}Fe is 327°C, while those of H in H_2O , O in UO_2 , and ^{238}U in UO_2 are 227°C. Instead of regenerating cross-section data for specific experimental conditions, multiple MCNP6 calculations have been conducted for the nearest temperature point and different temperature points, and the k_{eff} was obtained by interpolation. Table II shows the results of both the nearest temperature point and interpolated calculations. The RMS error of six cases drops from 0.25% δk to 0.12% δk when the k_{eff} is interpolated to the actual measured temperature.

2. Fission Reaction Rate

In the KRTIZ-2 experiments, the rod-to-rod fission rates were measured by gamma scanning. A single-reference rod from each experiment was chosen and repeatedly measured for the decay correction. Then, all measured fission rates of other rods were normalized to the reference rod. The DRAGON input models were reconstructed to extract fission rates for selected rods from the core calculation.

KRITZ-2:1. The calculation was conducted only at 248.5°C because the measured fission rates are not available at 19.7°C. Twenty-one fuel rods were selected for measurements with the reference rod at XY position (22, 23). The normalized fission rates are compared in Fig. 5 where rod number 16 is the reference rod. The difference between the measurement and DRAGON/PARCS simulation is mostly less than 4%. Rod number 2, which is located at the corner of the rectangular core, shows the largest discrepancy of 7.2%. Rod number 13 also shows a large discrepancy of fission rate, of which the measurement error is known to be

relatively large. For the DRAGON/PARCS, the maximum and RMS errors of the fission rates are 7.2% and 3.5%, respectively, while they are 6.1% and 2.9%, respectively, for the MCNP6 simulation.

KRITZ-2:13. This experiment has fission rate measurements for 30 fuel rods, with the reference rod at position (23, 22), or rod number 23 in Fig. 6. The distribution of fission rates for the cold condition is almost the same as that for the elevated temperature condition. However, the maximum and RMS errors are 8.6% and 3.9%, respectively, for the cold condition, while they are 10.8% and 5.0%, respectively, for the elevated temperature. The large error occurs for the rod, which is not surrounded by four fuel rods. For example, rod numbers 1, 3, 29, and 30 are at the corner position of the core, rod numbers 2 and 22 are on the side of the core. The MCNP6 calculations have relatively lower error when compared with the DRAGON/PARCS: 7.3% and 2.7% for the cold condition, and 4.7% and 2.2% for the elevated temperature condition.

KRITZ-2:19. This experiment has measurement data for 25 rods. There are no corner rods, but rod numbers 1 and 25 are on the core side. The reference fuel rod is at (14, 14) or rod number 12 in Fig. 7. The maximum and RMS errors of DRAGON/PARCS fission rates are 7.4% and 2.3%, respectively, for the cold condition, while they are 8.8% and 4.2%, respectively, for the elevated temperature condition. The prediction errors of MCNP6 calculations are slightly lower than those of DRAGON/PARCS: 5.4% and 1.5% for the cold condition and 6.7% and 4.1% for the elevated temperature condition.

In general, the error of fission rate prediction by DRAGON/PARCS is less than ~4% in the corner, and side rods are not included. This also indicates that the calculation results can improve if those fuel rods are separately treated in the model. The error of fission rate prediction by MCNP6 is in general less than that by DRAGON/PARCS by ~1%. However, in certain cases such as KRITZ-2:19, the prediction error of both DRAGON/PARCS and MCNP6 are off the reference values by the same amount, which could be due to the measurement uncertainty, i.e., ~1% (1σ) or higher.

TABLE II. Calculated effective core multiplication factors

	KRITZ-2:1 19.7°C	KRITZ-2:1 248.5°C	KRITZ-2:13 22.1°C	KRITZ-2:13 243.0°C	KRITZ-2:19 21.1°C	KRITZ-2:19 235.9°C
MCNP6 – Nearest temperature	0.99853 ±0.00007	0.99670 ±0.00008	1.00040 ±0.00008	0.99682 ±0.00007	1.00195 ±0.00008	0.99663 ±0.00008
MCNP6 - Interpolated	0.99856	0.99948	1.00036	0.99906	1.00199	0.99924
DRAGON/PARCS	0.99649	0.99544	0.99943	0.99606	0.99827	0.99214

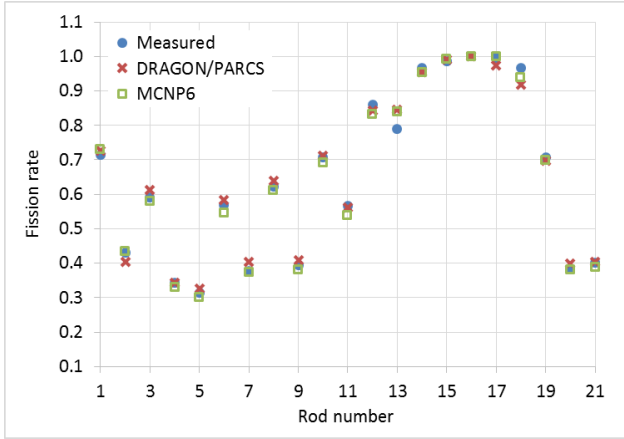
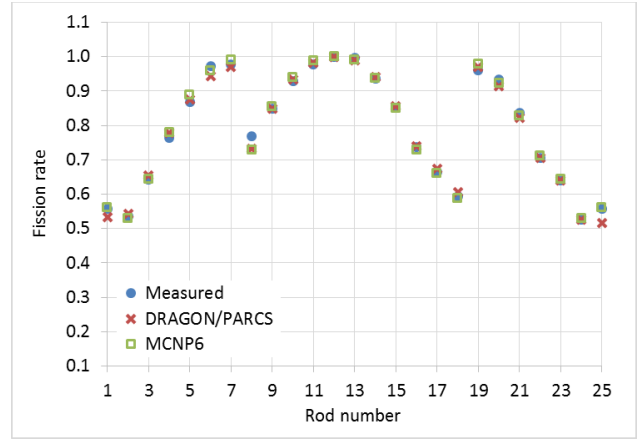
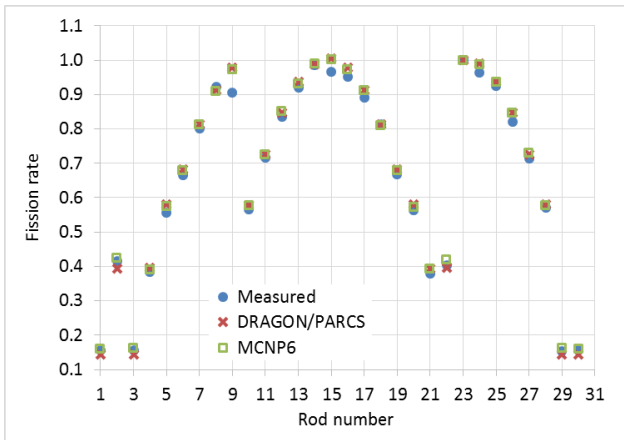


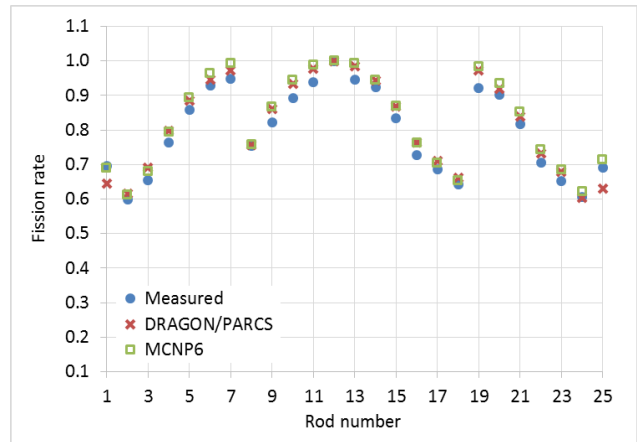
Fig. 5. Comparison of fission rates for KRITZ-2:1 at the elevated temperature.



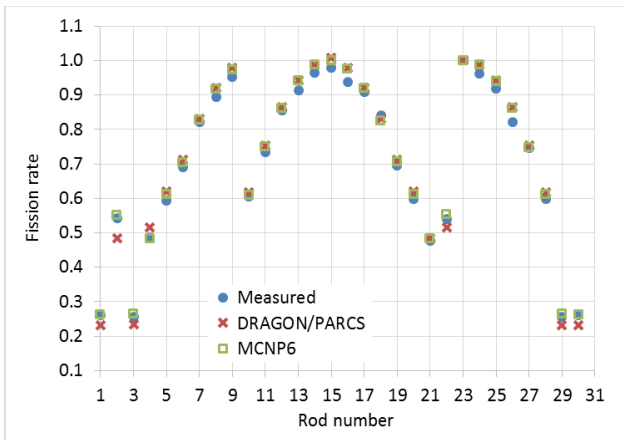
(a) KRITZ-2:19 cold condition



(a) KRITZ-2:13 cold condition



(b) KRITZ-2:19 elevated temperature



(b) KRITZ-2:13 elevated temperature

Fig. 6. Comparison of fission rates for KRITZ-2:13.

Fig. 7. Comparison of fission rates for KRITZ-2:19.

IV. CONCLUSION

In order to validate the DRAGON/PARCS system and computational model, the KRITZ-2 benchmark problems were revisited for criticality and fission reaction rate calculations. The PARCS core calculations with the 2-D DRAGON lattice models reproduce the criticality well. DRAGON/PARCS also predicts the fission rates mostly within ~4% for the fuel rods not on the core boundary. The MCNP6 results are in general consistent with DRAGON/PARCS results, but with less errors. There are several remarks regarding the results of present benchmark exercise as follows:

It is important to carefully treat the fuel rods located on the core boundary, which have a different neutron moderation effect when compared to the rest of fuel rods. Depending on the size of the problem, it may be required to model sub-lattices (smaller size lattice) for cross-section generation to get a better result.

In the present exercise, a shape function of the flux/power was obtained from the DRAGON model and used to reconstruct the fission rate using the assembly power from PARCS. In reality, the core is not symmetric, and the shape function could be slightly different for each assembly, but this effect is expected to be small.

It is expected that the effect of number of energy groups and group structure for DRAGON and PARCS is not significant for the thermal reactor problem, but is recommended to be confirmed.

ACKNOWLEDGEMENTS

This work was supported by General Atomics internal funding.

REFERENCES

1. G. MARLEAU, A. Hebert, R. Roy, "A User Guide for DRAGON Version 4," Technical Report IGE-294, École Polytechnique de Montréal, January 2016.
2. T. DOWNAR, Y. XU, V. SEKER, N. HUDSON, "PARCS v 3.0 U.S. NRC Core Neutronics Simulator User Manual," UM-NERS-09-0001, University of Michigan, September, 2013.
3. "Benchmark on the KRITZ-2 LEU and MOX Critical Experiments," NEA/NSC/DOC(2005)24, ISBN 92-64-02298-8, Organization for Economic Cooperation and Development, 2006.
4. Y. XU, B. COLLINS, T. DOWNAR, "GENPMAXS v.9: Program for Generating the PARCS Cross Section Interface File PMAXS," UM-NERS-09-004, University of Michigan, October 2009.
5. F. GIUST, R. STAMMLER, "HELIOS v 1.8 User Guide and Manual," Studsvik/Scandpower, 2003.
6. M. EDENIUS, A. AHLIN, "CASMO-3: New features, Benchmarking, and Advanced Applications," *Nucl. Sci. Eng.* 100, pp. 342-352, 1988.
7. M. DEHART et al., "TRITON: An Advanced Lattice Code for MOX Fuel Analysis," ANS Topical Meeting: Advances In Nuclear Fuel Management III, Hilton Head, Oct. 5-8, 2003.
8. J. L. CONLIN et al., "Continuous Energy Neutron Cross Section Data Tables Based upon ENDF/B-VII.1," LA-UR-13-20137, Los Alamos National Laboratory, February 2013.
9. F. LESZCZYNSKI, D. L. ALDAMA, A. TRKOV, "WIMS-D Library Update," International Atomic Energy Agency, May 2007.
10. M. A. ELSAWI, A. S. HRAIZ, "Benchmarking of the WIMS9/PARCS/TRACE code system for neutronic calculations of the Westinghouse AP1000™ reactor," *Nuclear Engineering and Design* 293 (2015) 249–257
11. R. CHAMBON, "Implementation of pin power reconstruction capabilities in the DRAGON5/PARCS

system," IGE-349, Ecole Polytechnique de Montreal, December 2015.